Geomechanics and Engineering, *Vol. 24, No. 4 (2021) 337-348*
DOI: https://doi.org/10.12989/gae.2021.24.4.337

Performance monitoring of offshore PHC pipe pile using BOFDA-based distributed fiber optic sensing system

Xing Zheng[1], Bin Shi*[1], Hong-Hu Zhu**[1], Cheng-Cheng Zhang[1,2], Xing Wang[3] and Meng-Ya Sun[1]

[1]*School of Earth Sciences and Engineering, Nanjing University, 163 Xianlin Ave, Nanjing, China*
[2]*Yuxiu Postdoctoral Institute, Nanjing University, 163 Xianlin Ave, Nanjing, China*
[3]*Nanjing University High-Tech Institute at Suzhou, 150 Renai Rd, Suzhou, China*

(Received July 21, 2020, Revised January 24, 2021, Accepted January 29, 2021)

Abstract. Brillouin Optical Frequency Domain Analysis (BOFDA) is a distributed fiber optic sensing (DFOS) technique that has unique advantages for performance monitoring of piles. However, the complicated production process and harsh operating environment of offshore PHC pipe piles make it difficult to apply this method to pile load testing. In this study, sensing cables were successfully pre-installed into an offshore PHC pipe pile directly for the first time and the BOFDA technique was used for in-situ monitoring of the pile under axial load. High-resolution strain and internal force distributions along the pile were obtained by the BOFDA sensing system. A finite element analysis incorporating the Degradation and Hardening Hyperbolic Model (DHHM) was carried out to evaluate and predict the performance of the pile, which provides an improved insight into the offshore pile-soil interaction mechanism.

Keywords: PHC pipe pile; Brillouin Optical Frequency Domain Analysis (BOFDA); offshore engineering; distributed fiber optic sensing (DFOS); load transfer analysis

1. Introduction

With the rapid development of marine economy and offshore engineering, prestressed high-strength concrete (PHC) pipe piles have been widely used in ports, docks, offshore platforms, and other offshore projects because of their unique advantages. The quality and deformation of PHC pipe piles are directly related to the stability and safety of the project. Therefore, it's very important to study the bearing behavior and the interaction between the pile and soil (API 2002, Baldwin *et al*. 2001, Feng *et al*. 2015, Xu *et al*. 2019).

The instrumented pile load test is the most reliable way to scientifically evaluate the bearing capacity of piles and master the law of pile-soil interaction (Chong 2019, Lehane and Jardine 1994, Seo *et al*. 2013). However, the research on the field test of offshore PHC pipe pile is very limited, because there are some difficulties in the applications of traditional point-type sensors (such as resistance strain gauges and vibrating wire sensors) and monitoring methods (Fellenius *et al*. 2004, Huang *et al*. 2008, Seo *et al*. 2013) of offshore instrumented load tests. Firstly, offshore PHC pipe piles need to penetrate into strata through the depth of seawater, so they are generally long and a lot of sensors and signal transmission lines are required, which will affect the integrity of the piles and increase the test cost. Secondly, it is a challenge for resistance sensors or vibrating wire sensors to survive the complicated production process and harsh operating environment of piles. Thirdly, because of the corrosive environment of the ocean, the durability of electrical or metal sensors is often difficult to meet the test requirements.

Distributed fiber optic sensing (DFOS) technique has unique advantages such as distributed, long-distance measurement, anti-corrosion, high precision and simple installation, providing a better solution for full-scale monitoring of piles (Bourne-Webb *et al*. 2009, Zhu *et al.* 2012, Mohamad *et al*. 2014, Moffat *et al*. 2015, Hong *et al*. 2016, Pelecanos *et al*. 2017 and 2018a, Shi *et al*. 2019, Wolfgang *et al*. 2011). Here, DFOS systems based on Brillouin backscattered principle are mostly used for strain/temperature measurement of piles (Gao *et al*. 2015 and 2019, Liu *et al*. 2017). Among them, Brillouin Optical Frequency Domain Analysis (BOFDA) technique has been continuously improved in last decade and demonstrated higher spatial resolution and accuracy, which is more suitable for performance monitoring of piles (Bao and Chen 2012, Gao *et al*. 2015, Nils *et al*. 2005 and 2019). However, BOFDA-based sensing system needs to measure from both ends of fiber optic (FO) cable. Once the FO cable breaks, it's difficult to repair, resulting in a great loss of material and manpower caused by the failure of the load test. Therefore, the installation and protection of FO cable for piles is an important issue.

For PHC pipe piles, the predecessors mostly used the method of slotting, embedding and then sealing by glue to install FO cables or FBG sensors on the pile surface (Kou *et al*. 2016a, b, Li *et al*. 2014, Lu *et al*. 2012). But this method is generally applicable to the detection of land foundation

*Corresponding author, Professor
E-mail: shibin@nju.edu.cn
**Corresponding author, Professor
E-mail: zhh@nju.edu.cn

ISSN: 2005-307X (Print), 2092-6219 (Online)

piles. For offshore PHC pipe piles, this method is difficult to ensure that the FO cables will not be destroyed during the transportation, hoisting of the foundation piles. The FO cables installed on the surface are also easily destroyed by sand and gravel in the hard stratums. In addition, this method is time-consuming and affects potentially the integrity of piles. Therefore, the installation and protection of FO cable for offshore PHC piles is still a challenge, which needs more attempts and practices to solve.

Combining a dock project of East Island in Zhanjiang City, China, this paper presents a case study of an in-situ experiment of an offshore PHC pipe pile. The FO cables were pre-installed into the PHC pipe pile during pile production process successfully to solve the difficulties of installation, which greatly improved the survival rate and test quality of the FO cables. Then, along with the offshore static load test, full-scale measurement of pile strain was conducted by BOFDA-based sensing system and the bearing behavior of piles are well analyzed based on field data. Finally, combined with DFOS data, a finite element analysis with Degradation and Hardening Hyperbolic Model (DHHM) was conducted for further understanding of the bearing behavior and pile-soil interaction. This research has important significance for the promotion of DFOS in the performance monitoring of offshore PHC pipe piles.

2. Measurement principle of pile stress and force based on BOFDA

2.1 Basic principle of BOFDA

Fig. 1 shows the basic principle of BOFDA. Similar to BOTDR and BOTDA, BOFDA also uses Brillouin backscattered light to detect the temperature or strain change of the optical fiber. A pump light and a probe light are injected into both ends of the sensing fiber, and when the two light waves meet, they will interact and excite acoustic wave. Acoustic wave acts as a medium to transfer energy from pump light to probe light. When the frequency difference Δf between the pump light and the probe light is equal to the fiber's local Brillouin frequency shift, the energy transmitted is the largest. A scan over Δf can search for the Brillouin frequency shift at every point of the fiber. Based on the linear relationship between the central frequency shift of the Brillouin backscattered light and the temperature or strain change of the optical fiber (Eq. (1)), the strain or temperature distribution along the fiber can be obtained (Agrawal 2001, Nikles and Thevenaz 1997).

$$\nu_B(\varepsilon, T) = \nu_B(\varepsilon_0, T_0) + C_1(\varepsilon-\varepsilon_0) + C_2(T-T_0) \quad (1)$$

where $\nu_B(\varepsilon_0, T_0)$ denotes the initial center frequency; ε and ε_0 denote the strain change in the optical fiber and the initial strain, respectively; T_0 and T denote temperature before and after straining or thermal change, respectively; C_1 denotes the strain coefficient, which is 0.05 MHz/με; and C_2 denotes the temperature coefficient and is 1.2 MHz/°C.

Compared to BOTDA and BOTDR, BOFDA has a unique baseband transfer function and deconvolution process, resulting in its higher spatial resolution and accuracy (Bernini *et al*. 2011, Kechavarzi *et al*. 2016, Zhang and Wu 2008). More details about the principle of BOFDA can refer to these papers (Bernini *et al*. 2011, Garcus and Gogolla 1997). An fTB-2505 BOFDA demodulator manufactured by fibrisTerre System GmbH was used in this research, and it can achieve ±2 με strain accuracy and 20 cm spatial resolution, which satisfies the requirements for pile testing.

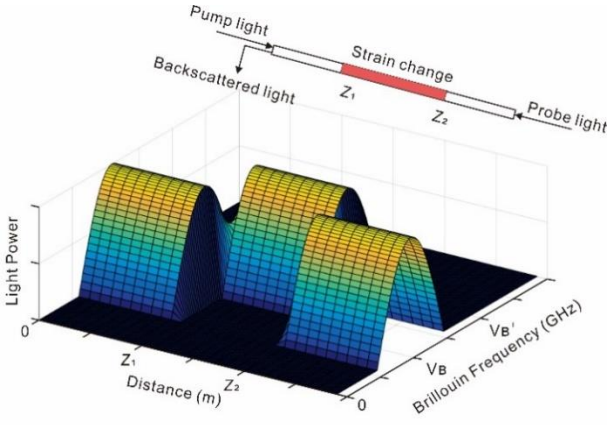

Fig. 1 Basic principle of BOFDA

2.1 Calculation of pile stress and force

Geotechnical performance of the pile is usually evaluated based on its axial force, shaft friction and tip resistance. The test pile can be divided into a series monitoring elements because of small sampling intervals of BOFDA-based sensing system. As long as the pile is installed with sensing cables correctly, the strain distribution of pile can be calculated using Eq. (1) based on the measured Brillouin frequency shifts. Then the axial force, shaft friction, and tip resistance of the pile can be calculated using the following equations (JGJ106-2014, Kechavarzi *et al*. 2019, Liu *et al*. 2017):

$$F_i = EA\overline{\varepsilon_i} \quad (2)$$

$$R_i = \frac{F_{i+1} - F_i}{\pi u l_i} \quad (3)$$

$$R_b = \frac{F_b}{A} \quad (4)$$

where F_i donates the axial force of the section of the pile; $\overline{\varepsilon_i}$ donates the average strain of the section S_i; E and A donate the Young's modulus and cross-sectional area of the pile, respectively; R_i and l_i donates the shaft friction and length between section i and section i+1, respectively; u donates the outer perimeter; R_b donates the tip resistance.

3. FO cable and installation

3.1 Cable description

FO cable is the essential sensing element and signal

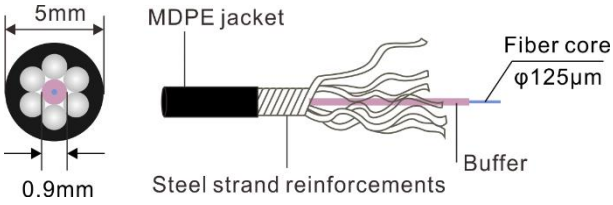

Fig. 2 Structure of the metal-reinforced FO cable

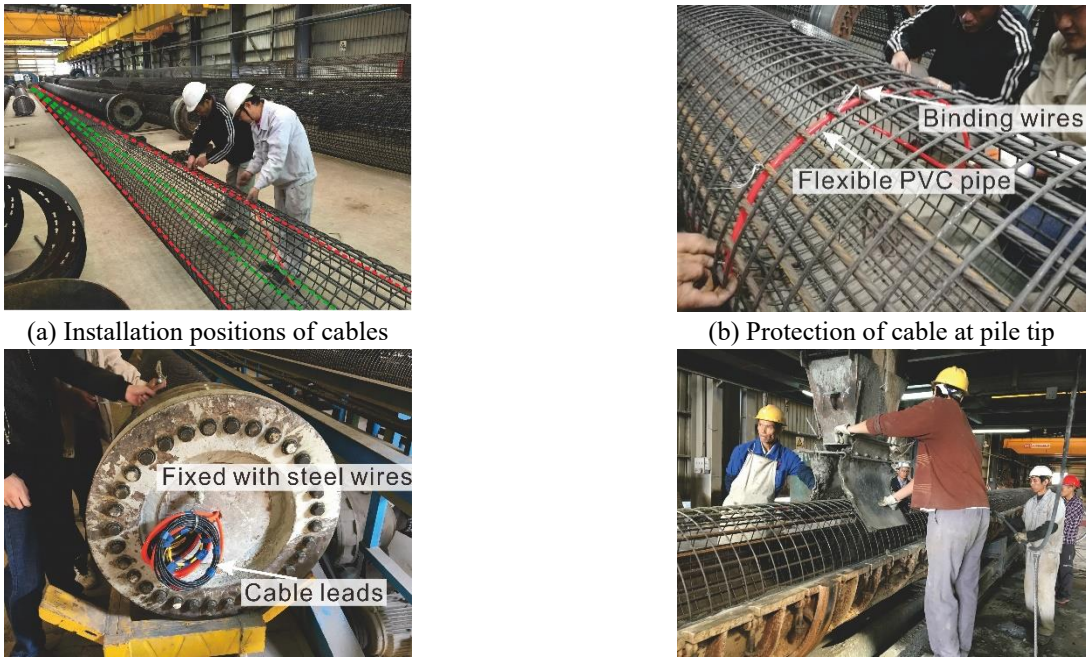

(a) Installation positions of cables

(b) Protection of cable at pile tip

(c) Protection of cable leads

(d) Pouring concrete to form pile

Fig. 3 Pre-installation of FO cables for PHC pipe pile

transmission medium of a DFOS system. Therefore, it is very important to choose an appropriate FO cable and installation method to ensure the survival and implantation quality. Due to the high-speed centrifugation and high-pressure steam curing processes during production of PHC pipe piles, common FO cables cannot withstand such a pile-making environment. In this study, a metal-reinforced strain sensing FO cable was used. The structure diagram of the cable is shown in Fig. 2. This sensing cable has high strength and good coupling with reinforced concrete and has been widely used in geological and geotechnical engineering monitoring or testing (Sun *et al*. 2014, Wang *et al*. 2017, Wu *et al*. 2017, Zhang *et al*. 2018a, b, 2019, 2021).

3.2 Pre-installation of cable

As mentioned earlier, it's difficult to meet the test requirements of offshore super long PHC piles using previous installation methods such as surface bonding or embedding in grooves. Therefore, the authors propose to install FO cables into the PHC pipe pile directly during pile production. The installation process is shown in Fig. 3, which is described as follows.

Four main rebars of the steel cage are selected symmetrically as the layout of FO cables (Fig. 3(a)). FO cables are pre-tensioned by 500-1000 με and are fixed directly on the rebars with steel wires. To avoid the damage at the pile tip during piling, the FO cables need to be protected by a flexible PVC pipe in the transition part of the pile bottom (Fig. 3(b)), and then continue to fix the cable on the symmetrical steel bar on the other side, thus forming a U-shaped loop. The redundant FO cables are reserved as lead wires on the top of the pile. The leads also need to be protected by PVC pipes and fixed to the outside of the mould with steel wires (Fig. 3(c)) to prevent damage during pile production, transportation and driving. Put the steel cage installed with FO cables into the mould, then pour the concrete and centrifuge the module at high speed (Fig. 3(d)). Finally, the FO cables become successfully embedded in the pile.

The pre-installation method of FO cables for PHC pipe piles is simple and free from the site and environment limitation. It ensures the survival rate of FO cables and does not affect the integrity of the pile. It can be applied to DFOS test of all PHC pipe piles.

4. Field testing

A dock project is proposed to be built in a bay on the east island of Zhanjiang City, China. It adopts an overlength PHC pipe pile as the form of foundation pile. To verify the

Table 1 Main parameters of test pile

Concrete grade	Total length (m)	Outer radius (m)	Wall thickness (m)	Young's modulus (GPa)
C80	52	0.6	0.13	53

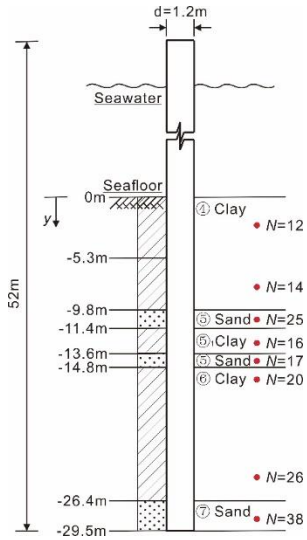

(a) Plan view and soil stratigraphy

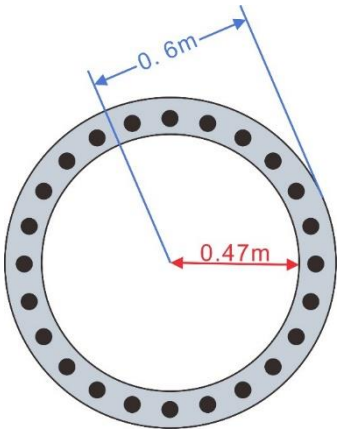

(b) Cross-section

Fig. 4 Test pile and soil stratigraphy

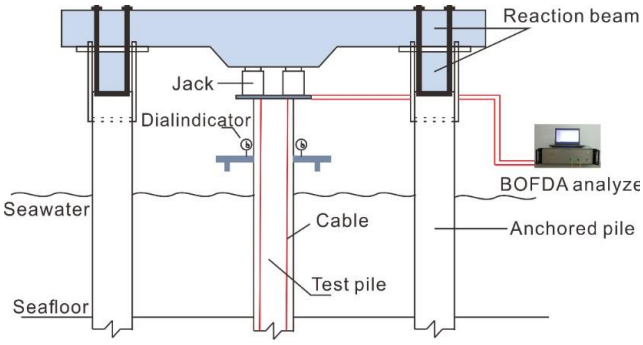

(a) Test apparatus

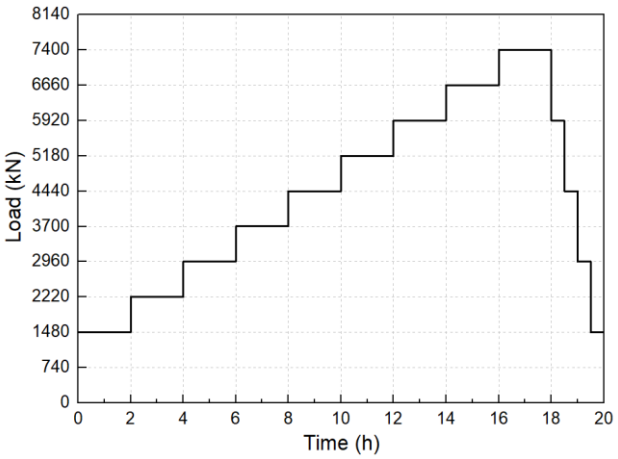

(b) Test schedule

Fig. 5 Offshore static load test

rationality of the foundation pile design, two test piles were selected for instrumented load test. FO cables were pre-installed into the piles in November 2016, and it is the first time to pre-installed FO cables into PHC pipe pile successfully. In this paper, only one of the large-diameter PHC pipe piles is selected as an example for analysis and discussion.

4.1 Test pile and soil stratigraphy

The PHC pile tested has a length of 52 m, a pile diameter of 1.2 m, and a wall thickness of 13 cm. The concrete number was C80 (Fig. 4). Table 1 shows the main parameters of the test pile. The test pile was driven to 29.5 m beneath the seabed and the local soil stratigraphy (Fig. 4(a)) consists of ④Clay, ⑤Sand (Medium-Coarse-Gravel sand), ⑤$_1$Clay with sand, ⑤Sand (Medium-Coarse-Gravel sand), ⑥Clay, and ⑦Sand (Medium-Coarse-Gravel sand). The results of the standard penetration test (SPT) are also shown in the Fig. 4(a) and the red points represent the test locations.

4.2 Offshore static load test

The anchored pile reaction method was used in the field test. As shown in Fig. 5(a), the test apparatus mainly consists of anchored piles, reaction beams, base beam, and hydraulic jacks. The hydraulic jacks exerted the load on the

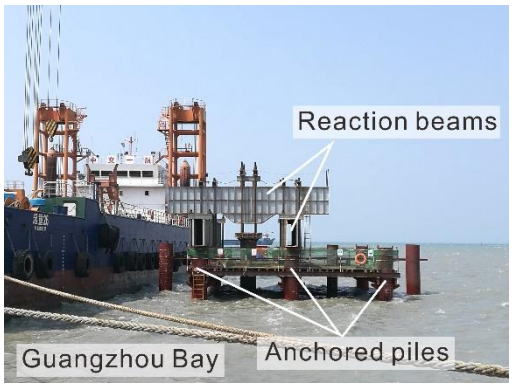

(a)

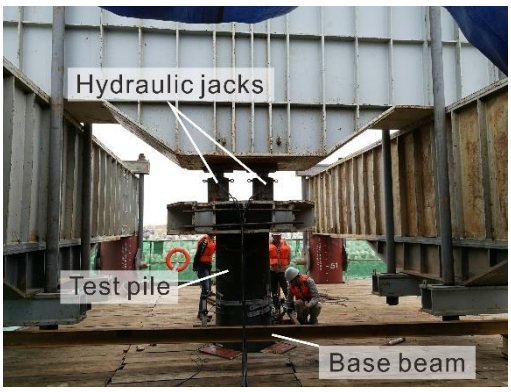

(b)

Fig. 6 Test site

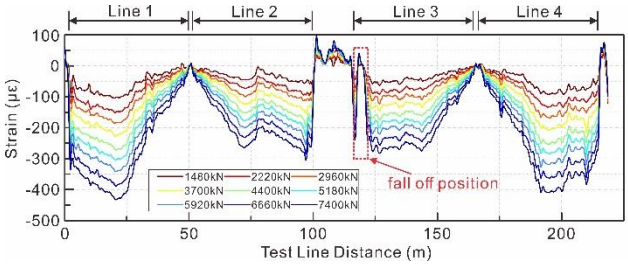

Fig. 7 Strain distribution along the FO cable

pile top through the reaction force provided by reaction beams and four anchored piles. The settlement of the pile top was obtained by the dial gauges arranged around the top pile body. The static load test plan (Fig. 5(b)) referred to the code (JTS167-4—2012). Each load stage was applied for 2 hours, and the load was from the initial value 1480 kN to a maximum of 7400 kN with a gradient of 740 kN. The situation of the test site is shown in the Fig. 6.

4.3 Strain measurement

When the arrangement of test apparatus was completed, the sensing cables were led out from the hole reserved on the test pile and connected to the instrument. Then the initial Brillouin frequency shift along the cable was measured by the BOFDA analyzer before the static load test. In this experiment, the spatial resolution of the instrument was set as 20 cm, and the sampling interval was 6.3 cm. During the static load test, the Brillouin frequency shift distribution under each load will be measured until the end of the test. According to Eq. (1), the strain distribution of the cables under each load can be obtained. In this study, only the data below 3 m above the sea level were used for further analysis, and the effect of temperature was relatively small, so no additional temperature compensation was made.

5. Test results

5.1 Strain distribution

Fig. 7 shows the strain change distribution along the FO cable under each load. The strain distribution curves (Fig. 7) indicate that the strain of FO cable increased steadily with the increase of the load, and decreased with the increase of the buried depth of the pile body. A section of strain at the top of Line 3 was almost 0, and a small section of FO cable had fallen off during the pile production. The asymmetry of strain curves indicates that eccentric load appeared in static load test. Therefore, average strain of four test lines was used as pile strain distribution for further analysis of pile stress to alleviate the influence of eccentric load (Kechavarzi *et al*. 2019, Liu *et al*. 2017, Lu *et al*. 2012).

The strain distribution of the pile (Fig. 8) can be divided into three parts: the pile strain in the soil part decreased gradually with the depth of the pile due to the effect of the shaft friction, and the pile strain in the seawater part was quite uniform. For that above the seawater, a section of the cable at the top of the pile detached from the pile during the pile production process, so the obtained strains were significantly small.

5.2 Bearing behavior

In this case, the Young's modulus and the cross-sectional area of the pile body are all fixed values, and the Young's modulus E is 53 GPa and the cross-sectional area A is 0.44 m^2. According to Eqs. (2)-(4), the curves of axial force and shaft friction (average value of each soil layer) under each load is shown in Fig. 9 and the shaft friction and tip resistance developed with top load are shown in Fig. 10.

Figs. 9 and 10 indicate that the top load was shared by the shaft friction and tip resistance. However, shaft friction bore most of the top load and the tip resistance only bore less than 10% of the top load under the maximum load. This

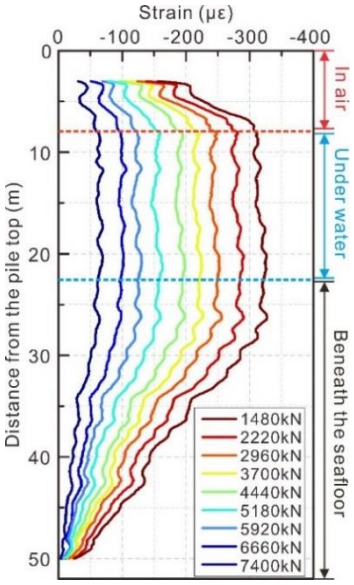

Fig. 8 Strain distribution of PHC pipe pile

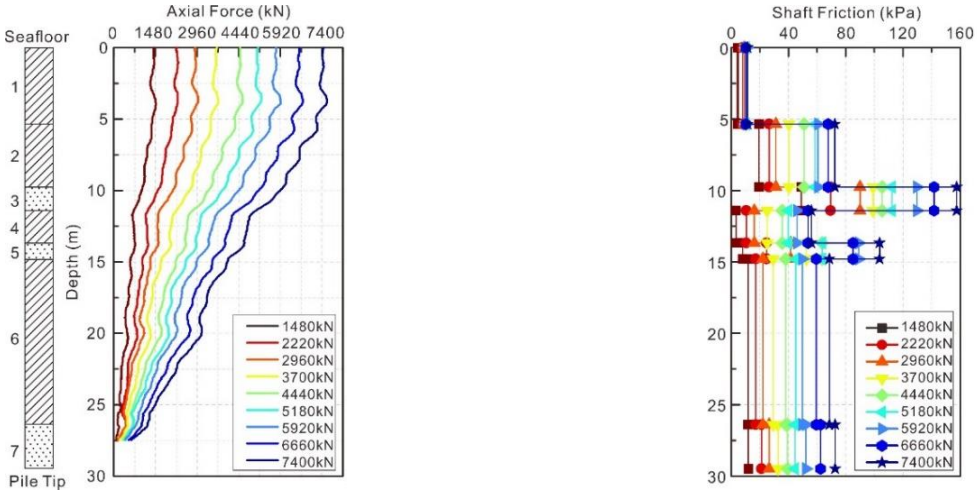

(a) (b)

Fig. 9 Curves of axial force (a) and shaft friction (b)

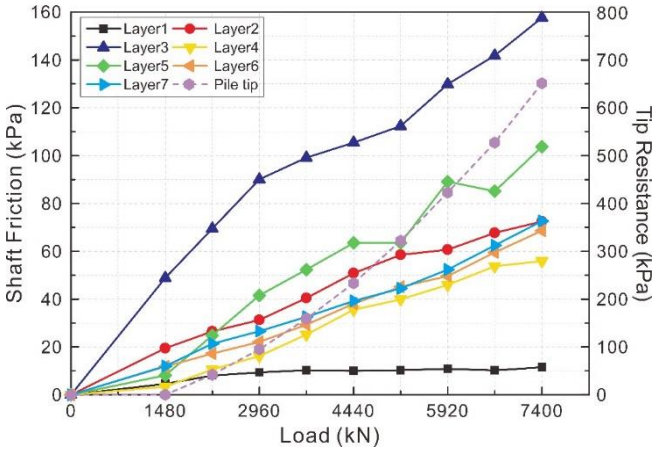

Fig. 10 Development of shaft friction and tip resistance of the pile with loads

test pile should be defined as an end-bearing friction pile. The tip resistance increased linearly with the increase of the load, but it was far smaller than the limit value given by geotechnical investigation report (8000 kPa). Although

Layer 1 and Layer 2 are both ④ Clay, Layer 1 has a lower density. Moreover, the upper pile body was disturbed by horizontal loads such as waves, so that the top layer is relatively loose, and even a gap was formed between the pile and soil. Moreover, the lubrication effect of the seawater reduced the shaft friction of Layer 1 (with a peak of ~11 kPa), which was much lower than that of Layer 2. Layer 3 and Layer 5 are both ⑤ Sand (Medium-Coarse-Gravel sand) with large shaft friction. Layer 4 ($⑤_1$ Clay with sand) in between them is a weak interlayer, and the shaft friction was significantly lower. Although the composition and origin of Layer 3 and Layer 5 are the same, the shaft friction of Layer 3 was significantly larger than that of Layer 5, and shaft friction under the maximum load reaches nearly 160 kPa. The site geology survey data shows that the SPT number of Layer 3 was N = 25, which was significantly larger than the N = 17 of Layer 5 (Fig. 4(a)), so this phenomenon is mainly caused by the difference in soil density. The slope of the shaft friction curves of Layer 2, 3, 4 gradually slowed down, indicating that the shaft friction of these soil layers is about to be fully realized. While the shaft friction of Layer 5, 6, 7 was still increasing, there is still a certain space from the recommended values of the geotechnical investigation report.

5.2 Vertical displacement

The strain distribution of the whole pile was obtained by BOFDA-based instrument, and the pile-soil relative displacement distribution curves were obtained according to Eq. (5), as shown in Fig. 11.

$$s(y) = s + \overline{\varepsilon_1} * y_1 + \int_0^y \overline{\varepsilon} dy \tag{5}$$

where y donates the depth from the seafloor; $s(y)$ donates the relative vertical displacement between the pile and soil at the depth y; s donates the settlement of pile top; $\overline{\varepsilon_i}$ donates the average strain of the pile above the seafloor (here, the average strain within 10-20m of the pile body in Fig. 8 was picked); y_i donates the distance from the pile top to the seafloor; $\overline{\varepsilon}$ donates the strain of pile at the depth y.

The test results indicate that: the pile load was mainly borne by the shaft friction of the upper layers at first. As the load increased, the compression of the upper pile body gradually increased, the relative vertical displacement gradually increased, and the shaft friction gradually developed completely and softened (like Layer 1). With the downward transfer of the load, the relative vertical displacement in the lower layers also increased gradually, and the shaft friction and the pile tip resistance gradually developed, but there was still a gap between field FO data and the limit value obtained from the geotechnical investigation. The internal force test of the pile and the analysis of the bearing characteristics show that the design of the test pile is conservative.

Field test results show that the implantation of FO cable and field experiments were successful. BOFDA technique can finely obtain the pile strain and internal force distribution, and can accurately obtain the axial force and shaft friction of the thinner stratum (such as Layer 5, its thickness is only 1.1 m). This study can provide valuable reference for PHC pipe pile, especially offshore long PHC pipe pile.

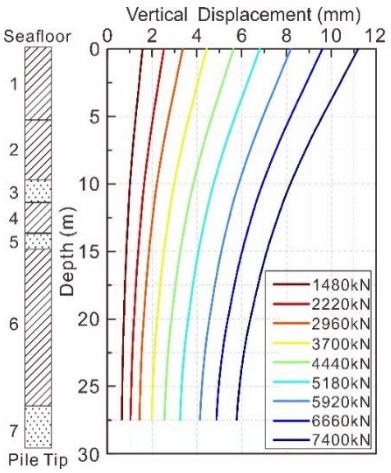

Fig. 11 Relative vertical displacement

6. Load transfer analysis with DHHM

Combined with DFOS data for offshore instrumented pile load test, a simple one-dimensional finite element model (Fig. 12) was established for better understanding of bearing behavior and pile-soil interaction. The 29.5 m PHC pipe pile under the seafloor is divided into hundreds elastic units with a length ΔL=0.126 m, which is twice the sampling interval used in the test. A set of nodes are arranged on the top and bottom sides of each pile unit, and the shaft friction and the tip resistance in the calculated length of the node are concentrated on the node, which is represented by a nonlinear spring. The nonlinear spring represents the relationship between the resistance R of the pile unit and the relative vertical displacement s, which was defined as load transfer function (Bohn *et al*. 2016, Chalmovsky and Mica 2020, Seed and Reese 1957). From the equilibrium condition of the force, it is not difficult to draw the Eq. (6):

$$([K_p]+[K_s])\{s\} = \{F\} \tag{6}$$

where $[K_p]$ and $[K_s]$ donate the global pile and soil stiffness matrices, respectively; $\{s\}$ donates the vector of the displacements and $\{F\}$ donates the vector of the externally applied forces. Here, the soil stiffness of each node can be obtained by comparing the total resistance in the node's calculated length with its relative displacement. For example, Eq. (7) shows the calculation of the soil stiffness of the pile tip:

$$k_{Sb} = \frac{\tau_b \cdot A + \tau_s \cdot u \cdot \frac{\Delta L}{2}}{S_b} \tag{7}$$

where k_{sb} is the soil stiffness of the pile tip; τ_b is the pile tip resistance; τ_s is the pile shaft friction; S_b is the relative

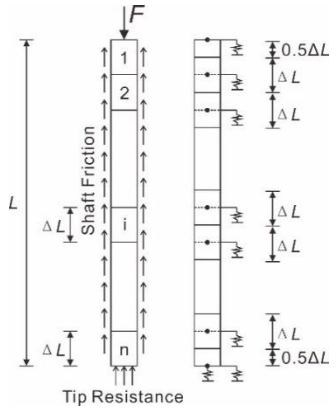

Fig. 12 Finite element analysis model

Table 2 Parameters of load transfer curves

	k_m (kN/m^2)	t_m (kN/m^2)	h	d
Layer 1	5433	11.5	1	1.6
Layer 2	15333	96.0	1	1.6
Layer 3	87914	138.0	0.8	1
Layer 4	9292	74.2	1	3
Layer 5	18625	120.0	1	3
Layer 6	15580	212.0	1	1
Layer 7	19498	182.2	1	1

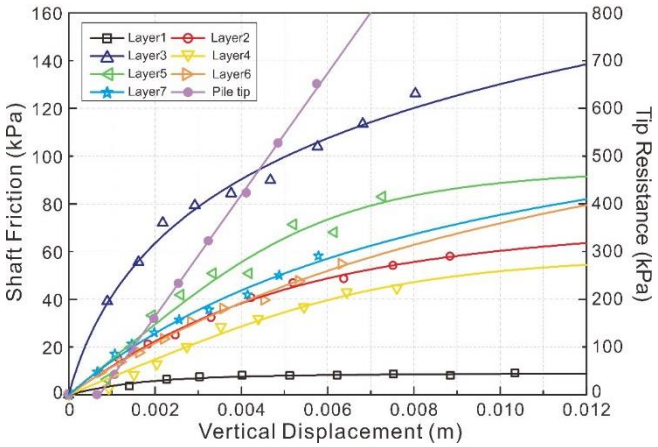

Fig. 13 Calibration of load transfer function parameters. Symbols represent field data; solid lines represent fitted load transfer function curves

vertical displacement at the pile tip.

Here, the DHHM load transfer function (Pelecanos *et al*. 2017, 2018a, b, Seo and Pelecanos 2018) was used in finite element analysis. The model is simple and can well express the hardening and softening effects of pile-soil interaction behavior. The model's expression is shown in Eq. (8):

$$\tau = \frac{k_m s}{d\sqrt[d]{(1+(\frac{k_m}{t_m}s)^{hd})}} \tag{8}$$

where k_m, t_m, h, and d are load transfer parameters. The physical meaning of these parameters is related to the hardening and creep properties of the soil, and can be obtained by fitting the measured results of the field test.

According to the FO data measured by BOFDA technique, the load transfer function parameters of each soil layer were obtained by fitting with the Levenberg-Marquardt algorithm in MATLAB which is shown in Table 2.

For the second and subsequent loading stages, the tip resistance had an approximately linear relationship with the relative vertical displacement, which can be expressed by Eq. (9):

$$\tau_b = 127.35*1000*s_b - 90.60 \tag{9}$$

The fitted load transfer curves are shown in Fig. 13.

After determining the model parameters of each layer,

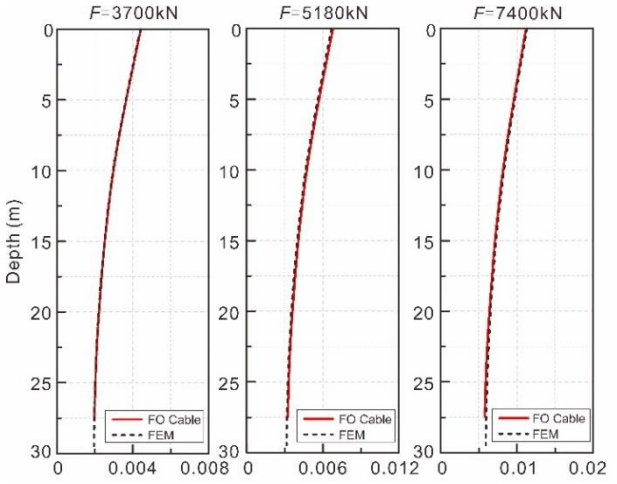

(a) Vertical displacement

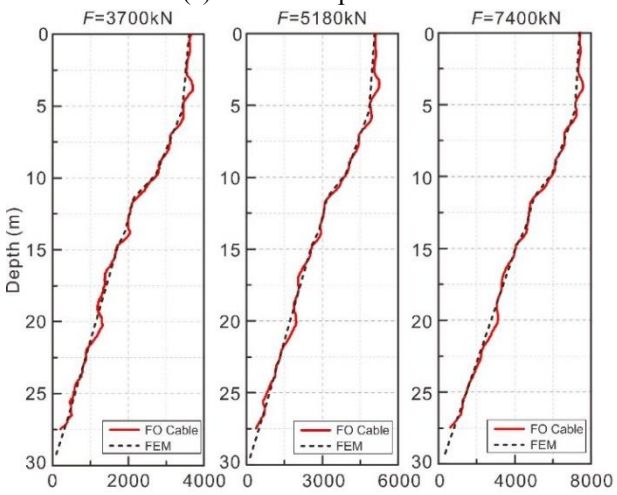

(b) Axial force

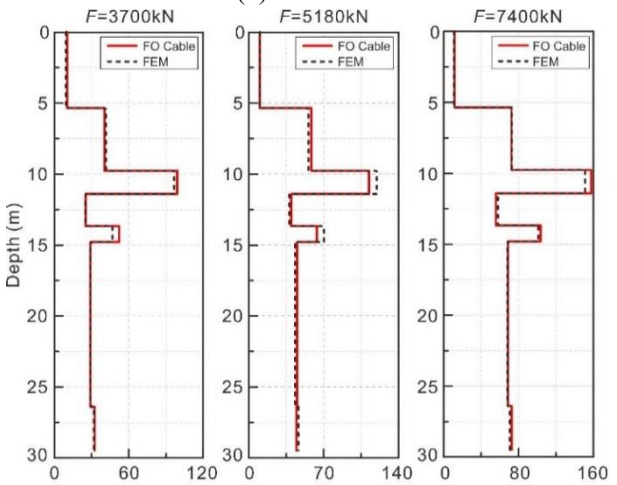

(c) Shaft friction

Fig. 14 Finite element analysis results

Eq. (6) was solved. The calculated relative displacement, axial force and shaft friction of the pile and the FO data are shown in Fig. 14.

Fig. 14 indicates that whether it is under low or high load, the finite element analysis results show good consistency with the FO cable data. The calculated vertical displacement differs from the actual measured data by a maximum of less than 0.2 mm. By back calculating with the vertical displacement, the axial force and shaft friction of the pile can be accurately obtained. Only when the load is large, the finite element analysis results of the shaft friction of Layer 3 and Layer 5 show a certain deviation, but still at a relatively low level. It can be obtained that the DHHM can establish the load transfer function between pile and

soil reasonably and accurately through the field data, which makes the numerical calculation results more reliable. The results can reflect the load transfer of test pile under vertical load and the law of pile-soil interaction. On the other hand, these results highlight the effectiveness and importance of distributed data along the pile in evaluating and predicting its geotechnical performance with DFOS system. Nowadays, the design value of the bearing capacity of the test pile is becoming much higher, and the cost of the static load test is also getting higher. Therefore, as long as the accurate load transfer curve parameters are obtained through the reliable field data, the vertical deformation and bearing capacity of the pile under higher load grade can be predicted, which can greatly save the test cost of the PHC pipe piles.

7. Conclusions

This paper presents a case study of in-situ monitoring of an offshore PHC pipe pile using a distributed fiber optic sensing system. During offshore static load test, full-scale measurement of the pile strain was carried out by the BOFDA technique, and the load transfer behavior of the pile under vertical loading was obtained. Based on field FO data, the finite element method with a novel load transfer function was used to numerically simulate the behavior of the test pile, and the following conclusions were drawn:

- The BOFDA technique has higher spatial resolution and accuracy, providing a distributed, high-precision and refined approach for performance monitoring of piles.
- A pre-installation method was proposed to solve the difficulties in protection and installation of FO cables on offshore PHC pipe piles. FO cables were installed into pile directly for the first time, and it is found that the proposed method is efficient and reliable.
- The test results indicate that the internal force distribution of the PHC pipe pile is closely related to the property of the soil around the pile. In this case, the vertical load was first taken up by the shaft friction of the upper layers. As the load increased, the shaft friction of Layer 1 appeared a peak of 11 kPa, and the shaft friction of Layers 2, 3 and 4 tended to slow down, while Layers 5, 6 and 7 and pile tip resistance still had space to develop, indicating that the design of the test pile was conservative.
- Based on distributed and high-resolution FO data, the accuracy of the DHHM load transfer model is improved, making the finite element analysis results more credible. The bearing mechanism of piles and the pile-soil interaction under high load can be predicted and analyzed.

The field study presented in this paper will provide a valuable reference for performance monitoring of PHC pipe piles, especially offshore overlength ones.

Acknowledgments

The authors gratefully acknowledge the financial supports provided by the National Natural Science Foundation of China (Grant No. 41427801) and Suzhou Science and Technology Development Plan: People's Livelihood Science and Technology (Grant No. SS201822). C.-C. Zhang was supported by the Yuxiu Young Scholars Program of Nanjing University (Grant No. 2010619). The authors also thank Xue-Qiang Gong, Wei Wang and CCCC Fourth Harbor Engineering Institute Co., Ltd. for their technical assistance.

References

Agrawal, G.P. (2001), *Nonlinear Fiber Optics* in *Nonlinear Science at the Dawn of the 21st Century*, Springer, Berlin, Heidelberg, Germany.

API RP 2A-WSD (2002), Planning, designing and constructing fixed offshore platforms—Working stress design, American Petroleum Institute, Washington, D.C., U.S.A.

Baldwin, C., Poloso, T., Chen, P. C., Niemczuk, J. B. and Ealy, C. (2001), "Structural monitoring of composite marine piles using fiber optic sensors", *Proceedings of the SPIE International Society for Optical Engineering*, Newport Beach, California, U.S.A., March

Bao, X. and Chen, L. (2012), "Recent progress in distributed fiber optic sensors", *Sensors*, **12**(12), 8601-8639. https://doi.org/10.3390/s120708601.

Bernini, R., Minardo, A. and Zeni, L. (2011), "Distributed sensing at centimeter-scale spatial resolution by BOFDA: Measurements and signal processing". *IEEE Photonics J.*, **4**(1), 48-56. https://doi.org/10.1109/JPHOT.2011.2179024.

Bohn C., Santos A.L.D. and Frank R. (2016), "Development of axial pile load transfer curves based on instrumented load tests", *J. Geotech. Geoenviron. Eng.*, **143**(1), 04016081. https://doi.org/10.1061/(ASCE)GT.1943-5606.0001579.

Bourne-Webb, P.J., Amatya, B., Soga, K., Amis, T., Davidson, C. and Payne, P. (2009), "Energy pile test at lambeth college, London: Geotechnical and thermodynamic aspects of pile response to heat cycles", *Geotechnique*, **59**(3), 237-248. https://doi.org/10.1680/geot.2009.59.3.237.

Chalmovsky, J. and Mica, L. (2020), "Prediction of the load-displacement response of ground anchors via the load-transfer method", *Geomech. Eng.*, **20**(4), 359-370. https://doi.org/10.12989/gae.2020.20.4.359.

Chong, S.H., Shin, H.S. and Cho, G.C. (2019), "Numerical analysis of offshore monopile during repetitive lateral loading", *Geomech. Eng.*, **19**(1), 79-81 https://doi.org/10.12989/gae.2019.19.1.079.

Fellenius, B.H., Harris, D.E. and Anderson, D.G. (2004), "Static loading test on a 45 m long pipe pile in sandpoint, idaho", *Can. Geotech. J.*, **41**(4), 613-628. https://doi.org/10.1139/t04-012.

Feng, S.J., Lu, S.F. and Shi, Z.M. (2015), "Field investigations of two super-long steel pipe piles in offshore areas", *Mar. Georesour. Geotec.*, **34**(6), 559-570. https://doi.org/10.1080/1064119X.2015.1038760.

Gao, L., Han, C., Xu, Z., Jin, Y. and Yan, J. (2019), "Experimental study on deformation monitoring of bored pile based on BOTDR", *Appl. Sci.*, **9**(12), 2435. https://doi.org/10.3390/app9122435.

Gao, L., Ji, B.Q., Kong, G.Q., Huang, X., Li, M.K. and Mahfouz, A.H. (2015), "Distributed measurement of temperature for PCC energy pile using BOFDA", *J. Sens.*, 1-6. https://doi.org/10.1155/2015/610473.

Garcus, D. and Gogolla, T. (1997), "Brillouin optical-fiber frequency-domain analysis for distributed temperature and strain measurements", *J. Lightwave Technol.*, **15**(4), 654-662.

https://doi.org/10.1109/50.566687.
Hong, C.Y., Zhang, Y.F. and Liu, L.Q. (2016), "Application of distributed optical fiber sensor for monitoring the mechanical performance of a driven pile", *Measurement*, **88**, 186-193. https://doi.org/10.1016/j.measurement.2016.03.052.
Huang, L.J., Lin, Y., Cai, J. and Zhou, W.Q. (2008), "Dynamic and static comparative analyses of settlements of overlength PHC pipe piles", *Rock Soil Mech*., **29**(2), 507-511 (in Chinese).
JGJ106-2014 (2014), Technical code for testing of building foundation piles, Ministry of Construction of the People's Republic of China, Beijing, China.
JTS167-4—2012 (2012), Chinese Code for Pile Foundation of Harbor Engineering, Ministry of Construction of the People's Republic of China, Beijing, China.
Kechavarzi, C., Pelecanos, L., Battista, N.D. and Soga, K. (2019), "Distributed fibre optic sensing for monitoring reinforced concrete piles", *Geotech. Eng. J. SEAGS AGSSEA*, **50**(2), 43-51.
Kechavarzi, C., Soga, K., Battista, N.D., Pelecanos, L. and Mair, R.J. (2016), *Distributed Fibre Optic Strain Sensing for Monitoring Civil Infrastructure*, Thomas Telford, London, U.K.
Kou, H. L., Guo, W. and Zhang, M.Y. (2016), "Field study of set-up effect in open-ended phc pipe piles", *Mar. Georesour. Geotechnol*., **35**(2), 208-215. https://doi.org/10.1080/1064119X.2015.1133742.
Kou, H.L., Chu, J., Guo, W. and Zhang, M.Y. (2016), "Field study of residual forces developed in pre-stressed high-strength concrete (PHC) pipe piles", *Can. Geotech. J*., **53**(4), 696-707. https://doi.org/10.1139/cgj-2015-0177.
Lehane, B.M. and Jardine, R.J. (1994), "Displacement-pile behaviour in a soft marine clay", *Can. Geotech. J.*, **31**(2), 181-191. https://doi.org/10.1139/t94-024.
Li, G.W., Pei, H.F., Yin, J.H., Lu, X.C. and Teng, J. (2014), "Monitoring and analysis of PHC pipe piles under hydraulic jacking using FBG sensing technology", *Measurement*, **49**(1), 358-367. https://doi.org/10.1016/j.measurement.2013.11.046.
Liu, B., Zhang, D. and Xi, P. (2017), "Mechanical behaviors of SD and CFA piles using BOTDA-based fiber optic sensor system: A comparative field test study", *Measurement*, **104**, 253-262. https://doi.org/10.1016/j.measurement.2017.03.038.
Lu, Y., Shi, B., Wei, G.Q., Chen, S.E. and Zhang, D. (2012), "Application of a distributed optical fiber sensing technique in monitoring the stress of precast piles", *Smart Mater. Struct*., **21**(11), 115011. https://doi.org/10.1088/0964-1726/21/11/115011.
Moffat, R.A., Beltran, J.F. and Herrera, R. (2015), "Applications of BOTDR fiber optics to the monitoring of underground structures", *Geomech. Eng*., **9**(3), 397-414. https://doi.org/10.12989/gae.2015.9.3.397.
Mohamad, H., Soga, K. and Amatya, B. (2014), "Thermal strain sensing of concrete piles using brillouin optical time domain reflectometry", *Geotech. Test. J.*, **37**(2), 20120176. https://doi.org/10.1520/GTJ20120176.
Nikles, M. and Thevenaz, L. (1997), "Brillouin gain spectrum characterization in single-mode optical fibers", *J. Lightwave Technol*., **15**(10), 1842-1851. https://doi.org/10.1109/50.633570.
Nils, N. and Stefan, V.D.M. (2019), "Distributed brillouin sensing for geotechnical infrastructure: Capabilities and challenges", *Geotech. Eng. J. SEAGS AGSSEA*, **50**(2), 8-12.
Nils, N., Aleksander, W., Katerina, K. and Elke, T. (2009), "A distributed fiber-optic sensing system for monitoring of large geotechnical structures", *Proceedings of the 4th International Conference on Structural Health Monitoring of Intelligent Infrastructure*, Zurich, Switzerland, June.
Pelecanos, L. and Soga, K. (2018b), "Development of load-transfer curves for axially-loaded piles using fibre-optic strain data, finite element analysis and optimisation", *Proceedings of the 9th European Conference on Numerical Methods in Geotechnical Engineering*, Porto, Portugal, June.
Pelecanos, L., Soga, K., Chunge, M.P., Ouyang, Y., Kwan, V., Kechavarzi, C. and Nicholson, D. (2017), "Distributed fibre-optic monitoring of an Osterberg-cell pile test in London", *Géotech. Lett*., **7**(2), 152-160. https://doi.org/10.1680/jgele.16.00081.
Pelecanos, L., Soga, K., Elshafie, M.Z.E.B., Battista, N.D., Kechavarzi, C. and Gue, C.Y., Ouyang, Y. and Seo, H.J. (2018a), "Distributed fiber optic sensing of axially loaded bored piles", *J. Geotech. Geoenviron. Eng*., **144**(3), 04017122.1-04017122.16. https://doi.org/10.1061/(ASCE)GT.1943-5606.0001843.
Rui, Y., Kechavarzi, C., O'Leary, F., Barker, C., Nicholson, D. and Soga, K. (2017), "Integrity testing of pile cover using distributed fibre optic sensing", *Sensors*, **17**(12), 2949. https://doi.org/10.3390/s17122949.
Seed H.B. and Reese L.C. (1957), "The action of soft clay along friction piles", *Trans. Am. Soc. Civ. Eng*., **122**, 731-754.
Seo, H., Prezzi, M. and Salgado, R. (2013), "Instrumented static load test on rock-socketed micropile", *J. Geotech. Geoenviron. Eng*., **139**(12), 2037-2047. https://doi.org/10.1061/(ASCE)GT.1943-5606.0000946.
Seo, H.J. and Pelecanos, L. (2018), "Finite element analysis of soil-structure interaction in soil anchor pull-out tests", *Proceedings of the 9th European Conference on Numerical Methods in Geotechnical Engineering*, Porto, Portugal, June.
Shi B., Zhang D. and Zhu H.H. (2019), *Distributed Fiber Optic Sensing for Geoengineering Monitoring*, Science Press, Beijing, China.
Sun, Y. J., Zhang, D., Shi, B., Tong, H.J. and Wang, X. (2014), "Distributed acquisition, characterization and process analysis of multi-field information in slopes", *Eng. Geol.*, **182**, 49-62. https://doi.org/10.1016/j.enggeo.2014.08.025.
Wang, X., Shi, B., Wei, G., Chen, S.E., Zhu, H. and Wang, T. (2017), "Monitoring the behavior of segment joints in a shield tunnel using distributed fiber optic sensors", *Struct. Control Health Monit.*, e2056. https://doi.org/10.1002/stc.2056.
Wolfgang, R., And, H. and Krebber, K. (2011), "Fiber-optic sensor applications in civil and geotechnical engineering", *Photonic Sensors*, **1**(3), 268-280. https://doi.org/10.1007/s13320-011-0011-x.
Wu J.H, Jiang H.T., Su J.W., Shi B., Jiang Y.H. and Gu K. (2015), "Application of distributed fiber optic sensing technique in land subsidence monitoring", *J. Civil Struct. Health Monit.*, **5**(5), 587-597. https://doi.org/10.1007/s13349-015-0133-8.
Xu, D. S., Xu, X. Y., Li, W. and Fatahi, B. (2020), "Field experiments on laterally loaded piles for an offshore wind farm", *Mar. Struct.*, **69**, 102684. https://doi.org/10.1016/j.marstruc.2019.102684.
Zhang, C.C., Shi, B., Gu, K., Liu, S.P., Wu, J.H. and Zhang, S., Zhang L., Jiang H.T. and Wei G.Q. (2018a), "Vertically distributed sensing of deformation using fiber optic sensing". *Geophys. Res. Lett*., **45**, 11732-11741. https://doi.org/10.1029/2018GL080428.
Zhang, C.C., Zhu, H.H., Liu, S.P., Shi, B. and Zhang, D. (2018b), "A kinematic method for calculating shear displacements of landslides using distributed fiber optic strain measurements", *Eng. Geol*., **234**, 83-96. https://doi.org/10.1016/j.enggeo.2018.01.002.
Zhang, H. and Wu, Z. (2008), "Performance evaluation of BOTDR-based distributed fiber optic sensors for crack monitoring", *Struct. Health Monit*., **7**(2), 143-156. https://doi.org/10.1177/1475921708089745.
Zhang, L., Shi, B., Zhu, H. Yu, X.B., Han, H. and Fan, X. (2021), "PSO-SVM-based deep displacement prediction of Majiagou landslide considering the deformation hysteresis effect", *Landslides*, **18**(1), 179-193.

https://doi.org/10.1007/s10346-020-01426-2.
Zhang, W., Xiao, R., Shi, B., Zhu, H.H. and Sun, Y.J. (2019), "Forecasting slope deformation field using correlated grey model updated with time correction factor and background value optimization", *Eng*. *Geol*., **260**, 105215. https://doi.org/10.1016/j.enggeo.2019.105215.
Zhu, H.H., Ho, A.N.L., Yin, J.H., Sun, H.W., Pei, H.F. and Hong, C.Y. (2012), "An optical fibre monitoring system for evaluating the performance of a soil nailed slope", *Smart*. *Struct*. *Syst*., **9**(5), 393-410. https://doi.org/ 10.12989/sss.2012.9.5.393.

GC